

# Hole in the Deuteron

Misak Sargsian

Florida International University, Miami, FL 33199

(Dated: October 14, 2024)

We introduce a new observable,  $A_{node}$ , that allows to isolate the node in the S-partial wave distribution of the deuteron in high  $Q^2$  electro-disintegration processes with tensor polarized target. The node is a signature of nuclear repulsive core and represents a crucial test of its strength, size as well as the role of the relativistic and non-nucleonic effects in a deeply bound state. Within plane wave impulse approximation the node immitates a “hole” through which incoming probe passes through without interaction. It is demonstrated that high  $Q^2$  electro-disintegration processes due to their strong anisotropy of final state interaction effects, allow to gain an unprecedented access to the node, opening up a new venue in probing elusive dynamics of the nuclear repulsive core.

**Introduction:** One of the most fascinating properties of nuclear forces is the nuclear repulsive core which provides a stability for atomic nuclei, making it possible the emergence of a structure for the visible matter[1]. Without it nuclei will collapse to sizes  $\sim 1$  fm, followed by the onset of quark-gluon degrees of freedom and restoration of chiral symmetry with rather unimaginable consequences for the order of the universe that we know.

**History of the Problem:** Already in 1950’s it was observed[2] that for the case of attractive two-nucleon forces the atomic nuclei with  $A \sim 200$  will collapse to the distances half of the  $NN$  interaction length, with per-nucleon binding energies  $\sim 1600$  MeV (compare to actual 8MeV). Moreover no saturation density is possible, with the nuclear binding energy growing as  $\sim A^2$ . Initially it was thought that the solution lies in the exchange character of nuclear forces as well as many-body effects[2]. However the solution came in 1950’s, from the theoretical analysis of the Berkeley 345 MeV pp scattering data which exhibited almost isotropic angular distribution for  $20^\circ - 90^\circ$  range of CM scattering angle. Such an isotropy was described by Jastrow[3, 4], by introducing a short range hard repulsive interaction, surrounded by an attractive well in the  $^1S_0$  channel of pp interaction. The further analyses of pn data demonstrated that similar repulsion exists also in  $^3S_1$  channel with the core distances estimated to be  $r_c \approx 0.4 - 0.6$  fm[5, 6].

**Current Status:** After seven decades, the dynamical origin of the repulsive core is as elusive as ever, providing little understanding why atomic nuclei are stable. The most modern  $NN$  potentials based on the fitting of phase-shifts still use the phenomenological ansatz for the repulsive core introduced in 1960’s. Attempts to describe the core through vector-meson exchanges face conceptual issues, mainly, on how to describe  $\leq 0.6$  fm inter-nucleon distances by the exchange of mesons with comparable or larger radii[7]. The situation is not better in effective theories in which short distance dynamics of NN interaction are absorbed in contact terms which are evaluated by comparing the calculations with low energy observables.

With the emergence of quantum chromodynamics (QCD), the studies of dynamical origin of the nuclear core obtained new dimensionality. QCD predicts robust inelastic transitions as well as sizable hidden color

component in the NN system at the core distances[8, 9]. One of the first attempts to explore the repulsive core in the S-channel of NN system was done within Lattice QCD[10], in which the obtained core confined at shorter distances ( $\lesssim 0.5$  Fm) and is much softer compared to the phenomenological potentials. The latter may be the reflection of the fact that no inelastic and hidden color components were included in the calculation. Further theoretical progress in calculating the core will require an inclusion of the hidden component in the NN system as well as accounting for the inelastic transitions - both imitate a repulsion due to orthogonality of these states with the detected  $NN$  states in the final state.

**Probing the NN Core:** The lack of progress is also related to the fact that there is very few processes (except perhaps the ones in the cores of neutron stars) that are directly related the dynamics of the nuclear core. The advance in understanding of the dynamical origin of the nuclear core will require relevant experimental data to be confronted with theoretical calculations. However at least three main challenges should be overcome in laboratory experiments in order to probe the nuclear core; (i) Experiments should provide sufficiently high energy and momentum transfer to reach the sub-fermi ( $\leq 0.6$  fm) distances in the  $NN$  system, (ii) Due to the nature of repulsion the experiments should be designed to measure diminishingly small cross sections, and (iii) Specific observables should be identified that are directly related to the dynamics of the nuclear core.

Never before the above three conditions were available in nuclear experiments. The situation is changed with 12 GeV energy upgrade of Jefferson Lab[11] which can provide high energy and high intensity electron beam for nuclear experiments.

The experimental approach in this case is to probe the  $^3S_1$  state in the deuteron or in short range  $pn$  correlations in nuclei. For the  $^1S_0$  state the repulsive core can be probed in short-range  $pp$  correlations in light nuclei. The methodology of these experiments is to consider high energy and momentum transfer electro-production reactions in which the detection of a struck nucleon from the deuteron (or struck and recoil nucleon from NN SRC) will allow to probe largest possible internal momenta in the NN system. The expectations in these experiments are

that for pn systems above 800 MeV/c internal momenta, the  ${}^3S_1$ -state starts to dominate the D-state, therefore the measured momentum distribution will be sensitive to the strength and the composition of the nuclear core. Indeed, the very first (and limited) measurement of high  $Q^2$  break-up of the deuteron at very high missing momenta,  $p_m$ , [12] observed that starting at  $p_m \geq 750$  MeV/c, the obtained momentum distribution is in qualitative disagreement with the predictions based on conventional wave functions of the deuteron. This can be the first indication of possible non-nucleonic components in the ground state wave function of the deuteron [13] that starts to dominate above the inelastic threshold of the isosinglet pn system. The discussed reaction is currently the most promising process in reaching the nuclear core and the analysis of the new data [14] may provide important new results. However the full theoretical analysis in this case, will require a reliable description of the  $D$ - wave at large internal momenta due to its contribution being large or comparable to the  $S$ - partial wave in the deuteron.

The alternative approach presented in this work, is to isolate S-wave contribution in the deuteron through the measurement of new kind of observable, referred to as  $A_{node}$  by using polarized deuteron target. The  $A_{node}$  should exhibit a node in the momentum distribution directly related to the dynamics of the repulsive core and as calculations show can be measured in exclusive deuteron break-up reactions at large  $Q^2$ .

**The NN Core and the Node in the S-State Distribution in the Deuteron:** We start with the simplistic discussion of the momentum distribution for  ${}^3S_1$  bound state in the deuteron in which potential is described (similar to Refs. [3, 6]) as a spherical well of radius  $R$  with infinite repulsive core at the center with radius  $R_c$  (Fig.1).

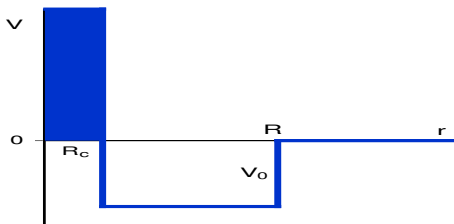


FIG. 1. Simple spherical well potential, with radius  $R$  and strength  $V_0$ , with infinite repulsive core at  $r \leq R_0$ .

In this case we consider not the pp scattering as in Ref. [3] but bound pn  ${}^3S_1$ -state with energy of the state matched to the deuteron bound state. Using Schroedinger equation we calculate the radial wave function,  $R_S(r)$  and then construct its momentum distribution as:

$$n(p) = |u(p)|^2, \text{ where } u(p) = \frac{2}{\sqrt{2\pi}} \int j_0(pr) R_S(r) r dr. \quad (1)$$

For the potential of Fig.1, the infinite core solution is  $R_S(r) = A \sin(k_0(R - R_c))$  for  $R_c \leq r \leq R$  and  $R_S(r) = B e^{-\kappa r}$ , for  $r > R$ , where  $k_0 = \sqrt{M(|E_b| + V_0)}$  and

$\kappa = \sqrt{M|E_b|}$ , with  $M$  and  $E_b$  being reduced mass and deuteron binding energy respectively. Applying continuity condition for the wave function and its first derivative and then using Fourier transform of Eq.(1) one obtains the momentum space radial wave function presented in Fig.2 (left panel) at different radii of the core.

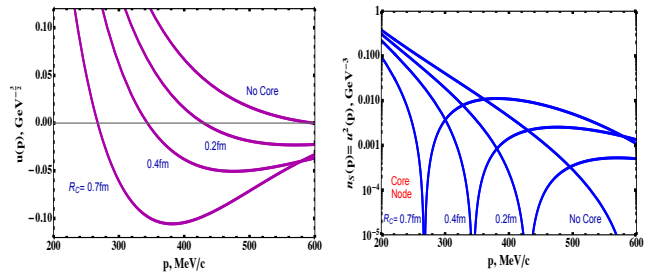


FIG. 2. (left)  ${}^3S_1$ - partial wave (left) and its momentum distribution (right) calculated for different sizes of the  $pn$  core.

As it is seen in the figure the momentum space wave function changes its sign, which is due to the sin function in the coordinate space with the boundary condition of the hard core  $R_S(R_c) = 0$ . The crossing zeros in  $R_S(r)$  correspond to the roots of transcendental equation with approximate relation for the crossing momentum:

$$p_0 \approx k_0 \left(1 - \frac{R_c}{R}\right) + \frac{\pi}{R} \left(1 - \frac{R_c}{R}\right)^2. \quad (2)$$

The crossing zero for the wave function in the momentum space will result in a node in the momentum distribution defined according to Eq.1 (Fig.2 (right panel)). These nodes are the reflection of the nuclear core that in the considered model are related the core's size.

Momentum distribution is a quantity which enters in the cross section of exclusive  $d(e, e'N_f)N_r$  processes in the plane wave impulse approximation (PWIA). In PWIA electron knocks out one of the nucleons from the deuteron without further re-interactions in the final state. If deuteron consisted of only the  $S$ -state, then in this case the node is like a *hole* in the momentum space through which the probe-electron will pass without interaction.

To see whether discussed simplistic model has a relevance for the realistic deuteron, in Fig.3 we present the momentum distribution of the nucleon in the deuteron calculated with realistic Paris [15], V18 [16] (hard) and CD-Bonn [17] (soft) NN potentials.

As the figure shows the S-wave momentum distribution indeed has a node and its position is related to the “hardness” of the NN potential. It is known that CD-Bonn potential is more soft predicting lesser high momentum component than the one with Paris and V18 potentials. However the realistic deuteron wave function also has a  $D$ - partial wave,  $w(p)$  and the actual momentum distribution is a sum of both S- and D- wave distributions:  $n(p) = |u(p)|^2 + |w(p)|^2$ . Because of this, as Fig.3 shows, Nature choose to hide the node of the S-wave momen-

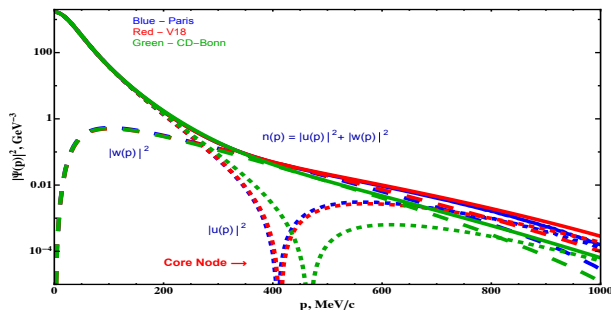


FIG. 3. Momentum distribution of partial  $S$  (dotted) and  $D$  (dashed) waves in the deuteron, as well as total momentum distribution (solid) for wave functions calculated with Paris, V18 and CD-Bonn potentials.

tum distribution by the robust  $D$ -wave distribution in the region of interest.

**Isolating S-wave Contribution:** The deuteron momentum distribution theoretically can be measured in above mentioned  $d(e, e', N_f)N_r$  reactions from unpolarized deuteron target within PWIA, in which it probes unpolarized deuteron density matrix:

$$\rho_{unp}(p) = n(p) = |u(p)|^2 + |w(p)|^2. \quad (3)$$

As Fig.3 shows in this case to be sensitive to the NN core one needs to measure very large internal momenta  $\geq 800$  MeV/C in which case  $S$ -wave distribution becomes comparable or exceeds that  $D$ -wave distribution. However, in this case, probing the core in the  $^3S$ -channel will not be direct due to the permanence of the  $D$ -wave contribution.

In this work an alternative approach is suggested which allows to maximally isolate  $S$ -state contribution by assuming simultaneous measurement of  $d(e, e', N_f)N_r$  reaction from unpolarized and tensor polarized deuteron.

The idea of using tensor polarized deuteron to probe the high momentum characteristics of the deuteron is more than half a century old. For the case of  $d(e, e', N_f)N_r$  reaction with tensor polarized deuteron it will probe the density matrix of the form:

$$\rho_{20}(p, \theta_N) \equiv \frac{|\psi_d^1|^2 + |\psi_d^{-1}|^2 - 2|\psi_d^0|^2}{3} = \frac{3 \cos^2(\theta_N) - 1}{2} \left[ 2\sqrt{2}u(p)w(p) - w^2(p) \right], \quad (4)$$

in which the  $S$ - partial wave contribution is suppressed (no  $|u(p)|^2$  term) allowing to explore the properties of  $D$ -partial wave. Here  $\psi_d^m$  represents the deuteron wave function with polarization  $m = -1, 0, 1$  and  $\theta_N$  is the direction of internal momenta with respect to the polarization axis of the deuteron.

Combining now Eqs.(3) and (4) in the form:

$$\begin{aligned} \rho_{node}(p) &= \rho_{unp}(p) + \frac{2\rho_{20}}{3 \cos^2(\theta_N) - 1} = \\ &= u^2(p) + 2\sqrt{2}u(p)w(p), \end{aligned} \quad (5)$$

one achieves an opposite effect in which  $|w(p)|^2$  does not enter and the combination will have a node corresponding to the crossing zero of the  $S$ -state wave function in momentum space.

It is more practical to consider a new asymmetry,  $A_{node}$  defined as:

$$\begin{aligned} A_{node}(p) &\equiv \frac{\rho_{node}(p)}{\rho_{unp}(p)} = 1 + \frac{2A_{zz}(p, \theta_N)}{3 \cos^2(\theta_N) - 1} \\ &= \frac{u^2(p) + 2\sqrt{2}u(p)w(p)}{u(p)^2 + w(p)^2}, \end{aligned} \quad (6)$$

where  $A_{zz} = \frac{\rho_{20}}{\rho_{unp}}$ , which within PWIA corresponds to the ratio of cross sections of  $d(e, e', N_f)N_r$  scattering from tensor polarized and unpolarized deuteron target:

$$T_{20} = \frac{\sigma_{tensor}}{\sigma_{unp}}. \quad (7)$$

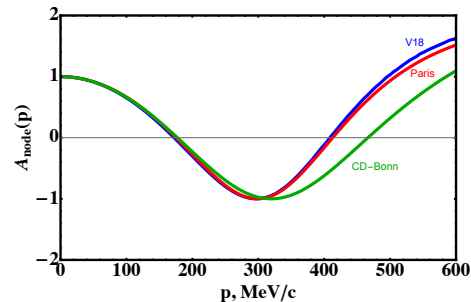


FIG. 4. Calculations  $A_{node}(p)$  using deuteron wave function calculated with Paris (red), CD-Bonn (green) and V18 (blue) potentials.

In Fig.4 asymmetry  $A_{node}(p)$  is calculated for  $\theta_N = 0$ . It shows large sensitivity of the node positions at  $p \geq 400$  MeV/c, to the choice of the NN potentials with which deuteron wave functions are calculated. This is consistent with  $S$ -state momentum distributions in Fig.3.

Note that  $A_{node}$  has another zero at  $p \approx 180$  MeV/c which corresponds to the condition of

$$u(p) = -2\sqrt{2}w(p). \quad (8)$$

Since the above relation takes place at relatively small internal moments for which the deuteron wave function is well known, the observation of this node will help to calibrate the experimental measurement of  $A_{node}$ .

**Feasibility of the  $A_{node}(p)$  Measurement:** Few decades ago the above discussion on possibility of isolating the  $S$ -state of the deuteron would have been purely theoretical, since low energy  $d(e, e', N_f)N_r$  experiments with  $Q^2 < 1$  GeV<sup>2</sup> were completely dominated by non-PWIA contributions such as recoil production of final nucleon, Final State Interactions (FSI), Meson-Exchange currents (MEC) and Isobar Contribution(IC)[18, 19]. As a result it was impossible to establish direct connection between internal momentum of the deuteron and measured momenta of scattered electron and nucleon,  $N_f$ .

This situation changed significantly with the emergence of high energy and intensity electron beam at Jefferson Lab which made it possible to measure at  $Q^2 > few \text{ GeV}^2$ . In this case, choosing momentum of the final nucleon comparable with the transferred large momentum,  $\mathbf{q}$  it was possible to identify clearly the final nucleon as the one which was struck by the virtual photon. The large  $Q^2$  allows to suppress MEC contribution and charge-interchange FSI, and finally the possibility of measuring at the kinematics of Bjorken  $x > 1$  (away from inelastic threshold) allowed to suppress the intermediate state Isobar contribution. As a result in high  $Q^2$  only PWIA and direct FSI processes contribute to the  $d(e, e', N_f)N_r$  reaction, Fig.5 (upper panel).

Another important advantage of high energy kinematics is the onset of the eikonal regime of the scattering. There was an intensive theoretical research in calculating the  $d(e, e', N_f)N_r$  reaction in eikonal approximation[20–26]. One of such approaches was the generalized eikonal approximation (GEA) which developed an effective Feynman diagrammatic rules for calculation of the nuclear scattering amplitude. Within GEA one calculates all contributions[20, 21, 25] to the nuclear scattering amplitude. For the simplicity of discussion we present the GEA predictions for dominant amplitudes only, which are PWIA,  $A_0^\mu$  and single rescattering,  $A_1^\mu$  terms:

$$\langle s_f, s_r | A_0^\mu | s_d \rangle = \sqrt{2} \sqrt{(2\pi)^3 2E_r} \times \sum_{s_i} J_N^\mu(s_f, p_f; s_i, p_i) \Psi_d^{s_d}(s_i, p_i, s_r, p_r), \quad (9)$$

$$\begin{aligned} \langle s_f, s_r | A_1^\mu | s_d \rangle &= \\ &= \frac{i\sqrt{2}(2\pi)^{\frac{3}{2}}}{4} \sum_{s'_f, s'_r, s_i} \int \frac{d^2 p'_r}{(2\pi)^2} \frac{\sqrt{s(s-4m^2)}}{\sqrt{2\tilde{E}'_r |q|}} \\ &\times \langle p_f, s_f; p_r, s_r | f^{NN, on}(t, s) | \tilde{p}'_r, s'_r; \tilde{p}'_f, s'_f \rangle \\ &\times J_N^\mu(s'_f, p'_f; s_i, \tilde{p}'_i) \cdot \Psi_d^{s_d}(s_i, \tilde{p}'_i, s'_r, \tilde{p}'_r) \\ &- \frac{(2\pi)^{\frac{3}{2}}}{\sqrt{2}} \sum_{s'_f, s'_r, s_i} \mathcal{P} \int \frac{dp'_{r,z}}{2\pi} \int \frac{d^2 p'_r}{(2\pi)^2} \frac{\sqrt{s(s-4m^2)}}{\sqrt{2\tilde{E}'_r |q|}} \\ &\times \frac{\langle p_f, s_f; p_r, s_r | f^{NN, off}(t, s) | p'_r, s'_r; p'_f, s'_f \rangle}{p'_{r,z} - \tilde{p}'_{r,z}} \\ &\times J_N^\mu(s'_f, p'_f; s_i, p'_i) \cdot \Psi_d^{s_d}(s_i, p'_i, s'_r, p'_r), \end{aligned} \quad (10)$$

where all momenta are defined in Fig.5. Here,  $s = (p_f + p_r)^2$ ,  $m$  is the nucleon mass,  $\tilde{p}'_r = (p_{r,z} - \Delta, p'_{r,\perp})$ ,  $\tilde{E}'_r = \sqrt{m^2 + \tilde{p}'_r{}^2}$ ,  $\tilde{p}'_i = p_d - \tilde{p}'_r$  and  $\tilde{p}'_f = \tilde{p}'_i + q$  and

$$\Delta = \frac{q_0}{|q|} (E_r - E'_r) + \frac{M_d}{|q|} (E_r - E'_r) + \frac{p_r'^2 - m^2}{2|q|}. \quad (11)$$

Above,  $J_N^\mu$  is the electromagnetic current of bound nucleon calculated within virtual nucleon approximation[25] and the deuteron wave function is defined at initial relative momenta of  $pn$  system. The on-shell part of the  $pn$  scattering amplitude,  $f^{NN, on}(t, s)$

is taken from experiments, while the off-shell counterpart is modeled as follows:

$$f^{NN, off} = f^{NN, on} e^{B(m_{off}^2 - m^2)}, \quad (12)$$

where  $m_{off}^2 \equiv (p'_f)^2$ . Note that the rendered uncertainty due to Eq.(12) is very small since principal value part of the rescattering amplitude is parameterically small.

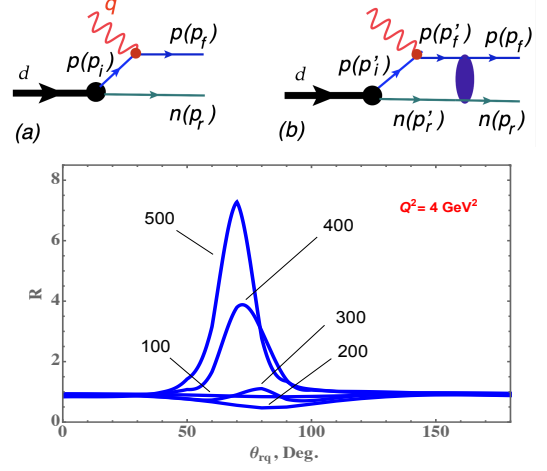


FIG. 5. (Upper panel) (a) PWIA and (b) direct FSI contributions to  $d(e, e', N_f)N_r$  reaction in eikonal approximation. (Lower panel) The  $\theta_{rq}$  dependence of the ratio ( $R$ ) of calculated cross section with FSI to the PWIA cross section, for different values of missing momenta at  $Q^2 = 4 \text{ GeV}^2$ .

With  $A_0^\mu$  and  $A_1^\mu$  the differential cross section for  $s_d$  polarized deuteron can be written as follows

$$\frac{d\sigma^{s_d}}{dE'_e, d\Omega_{e'} dp_f d\Omega_f} = \frac{\alpha^2 E'_e}{Q^4 E_e} \times \frac{1}{2} \sum_{s_f, s_r, s_1, s_2} \frac{|J_e^\mu J_{d,\mu}|^2}{2M_d E_f} \frac{p_f^2}{\left| \frac{p_f}{E_f} + \frac{p_f - q \cos(\theta_{p_f, q})}{E_r} \right|} \quad (13)$$

where  $E_e$  and  $E'_e$  are energies of the incoming and scattered electrons,  $\alpha$  is the Fine Structure constant. Here  $J_e^\mu$  is the leptonic current and  $J_d^\mu$  is the electromagnetic transition current of the polarized deuteron defined as

$$J_d^\mu = \frac{\langle s_f, s_r | A_0^\mu + A_1^\mu | s_d \rangle}{\sqrt{2(2\pi)^3 2E_r}}. \quad (14)$$

The presented GEA approach successfully described the data emerging from high  $Q^2$  experiments with unpolarized deuteron targets from JLAB, for recoil nucleon momenta up to 550 MeV/c (see e.g. Refs.[12, 27–29]). One of the important results in theoretical analysis of these data is the confirmation of strong angular anisotropy of FSI effects in which the rescattering is concentrated at the transverse kinematics of recoil nucleon angle with respect to the direction of momentum transfer  $q$ ,  $60^\circ \leq \theta_{rq} \leq 90^\circ$  (Fig.5). As Fig.5 (lower panel) shows, where  $R$  is the ratio of calculated cross



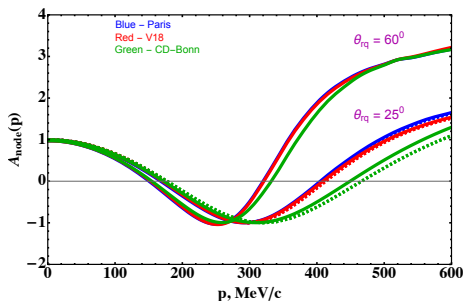


FIG. 6. Calculations  $A_{node}(p)$  using deuteron wave functions calculated with Paris (blue), CD-Bonn (green) and V18 (red) potentials for  $Q^2 = 4 \text{ GeV}^2$  and  $\theta_{rq} = 60^\circ$  and  $\theta_{rq} = 25^\circ$  recoil angles. Solid line for calculation including FSI, dashed line PWIA calculation.

section with  $A_0^\mu + A_1^\mu$  to the PWIA cross section, this anisotropy can be used to identify kinematics most optimal for probing internal structure of the deuteron with small correction due to FSI effects. This corresponds to the  $\theta_{min} < \theta_{rq} < 50^\circ$ , where  $\theta_{min}$  is defined by the minimal value of the relative momentum in the final  $pn$  system for which eikonal approximation is valid. The suppression of FSI in this region is confirmed by comparison with the large  $Q^2$  data[12, 28, 29]. It is worth mentioning that similar criteria can be used also for semi-exclusive processes involving other targets[30].

In Fig.6 the calculation of  $A_{node}$  is presented for  $Q^2 = 4 \text{ GeV}^2$  for kinematics of large and small FSI. As the

figure shows for the kinematics of large FSI ( $\theta_{rq} = 60^\circ$ ) different wave functions predict close values for  $A_{node}$ , which is expected due to the fact that FSI amplitude is dominated by small initial momenta for which different deuteron wave functions are similar. However for suppressed FSI kinematics ( $\theta_{rq} = 25^\circ$ ) the results are close to the PWIA prediction thus allowing direct probe of the node related to the repulsive core in the  $^3S_1$  channel.

**Summary and Outlook:** We suggested new observable  $A_{node}$  that isolates  $^3S_1$  state in the deuteron whose node in the momentum distribution is related to the strength of  $pn$ -repulsive core. The study of such a structure becomes possible with the emerging reality of high momentum transfer deuteron electro-disintegration reactions for which eikonal regime of FSI allows to isolate kinematics dominated by PWIA. Such studies will use also the development of new technologies which allow to employ polarized deuteron target with intensive electron beams[31, 32].

It is worth mentioning that our goal was not to discuss which model of deuteron wave function or (including relativistic and non-nucleonic effects) are valid but to demonstrate that it is possible to isolate the  $^3S_1$ - $pn$  state that will allow direct exploration of the repulsive core. Such an experiment is currently feasible albeit expensive, however no alternative experiments exist or planned for addressing decades long problem of understanding the nature of the nuclear repulsive core.

**Acknowledgment:** This work is supported by United States DOE grant under contract DE-FG02-01ER41172.

- 
- [1] F. Wilczek, *Nature* **445**, 156 (2007).  
[2] J. M. Blatt and V. F. Weisskopf, *Theoretical nuclear physics* (Springer, New York, 1952).  
[3] R. Jastrow, *Phys. Rev.* **79**, 389 (1950).  
[4] R. Jastrow, *Phys. Rev.* **81**, 165 (1951).  
[5] R. A. Arndt and M. H. Mac Gregor, *Phys. Rev.* **141**, 873 (1966).  
[6] J. D. Walecka, *Theoretical nuclear and subnuclear physics*, Vol. 16 (1995).  
[7] R. P. Feynman, *Photon-hadron interactions (Frontiers in Physics)* (Perseus, 1998).  
[8] M. Harvey, *Nucl. Phys. A* **352**, 326 (1981).  
[9] C. Ji and S. Brodsky, *Phys. Rev. D* **34**, 1460 (1986).  
[10] N. Ishii, S. Aoki, and T. Hatsuda, *Phys. Rev. Lett.* **99**, 022001 (2007), arXiv:nucl-th/0611096.  
[11] J. Dudek *et al.*, *Eur. Phys. J. A* **48**, 187 (2012).  
[12] C. Yero *et al.* (Hall C), *Phys. Rev. Lett.* **125**, 262501 (2020), arXiv:2008.08058 [nucl-ex].  
[13] M. M. Sargsian and F. Vera, *Phys. Rev. Lett.* **130**, 112502 (2023), arXiv:2208.00501 [nucl-th].  
[14] W. U. Boeglin *et al.*, Jefferson-Lab-Experiment-E12-10-003 (2014), arXiv:1410.6770 [nucl-ex].  
[15] M. Lacombe, B. Loiseau, R. Vinh Mau, J. Cote, P. Pires, and R. de Tourreil, *Phys. Lett. B* **101**, 139 (1981).  
[16] R. B. Wiringa, V. G. J. Stoks, and R. Schiavilla, *Phys. Rev. C* **51**, 38 (1995), arXiv:nucl-th/9408016.  
[17] R. Machleidt, *Phys. Rev. C* **63**, 024001 (2001).  
[18] H. Arenhovel, *Nucl. Phys. A* **384**, 287 (1982).  
[19] W. Boeglin and M. Sargsian, *Int. J. Mod. Phys. E* **24**, 1530003 (2015), arXiv:1501.05377 [nucl-ex].  
[20] L. L. Frankfurt, M. M. Sargsian, and M. I. Strikman, *Phys. Rev. C* **56**, 1124 (1997), arXiv:nucl-th/9603018.  
[21] M. M. Sargsian, *Int. J. Mod. Phys. E* **10**, 405 (2001).  
[22] S. Jeschonnek and J. W. Van Orden, *Phys. Rev. C* **78**, 014007 (2008), arXiv:0805.3115 [nucl-th].  
[23] J. M. Laget, *Phys. Lett. B* **609**, 49 (2005).  
[24] C. Ciofi degli Atti and L. P. Kaptari, *Phys. Rev. C* **71**, 024005 (2005), arXiv:nucl-th/0407024.  
[25] M. M. Sargsian, *Phys. Rev. C* **82**, 014612 (2010).  
[26] W. P. Ford, S. Jeschonnek, and J. W. Van Orden, *Phys. Rev. C* **87**, 054006 (2013), arXiv:1304.0647 [nucl-th].  
[27] K. Egiyan *et al.* (CLAS Collaboration), *Phys. Rev. Lett.* **98**, 262502 (2007), arXiv:nucl-ex/0701013 [nucl-ex].  
[28] W. U. Boeglin *et al.* (Hall A), *Phys. Rev. Lett.* **107**, 262501 (2011), arXiv:1106.0275 [nucl-ex].  
[29] W. U. Boeglin and M. M. Sargsian, *Phys. Lett. B* **854**, 138742 (2024), arXiv:2402.13411 [nucl-th].  
[30] M. M. Sargsian, T. V. Abrahamyan, M. I. Strikman, and L. L. Frankfurt, *Phys. Rev. C* **71**, 044615 (2005).  
[31] K. Slifer and E. Long, *PoS PSTP2013*, 008 (2013).  
[32] A. Accardi *et al.*, *Eur. Phys. J. A* **60**, 173 (2024).